miR-342-5p promotes *Zmpste24*-deficient mouse embryonic fibroblasts proliferation by suppressing GAS2

CHUN-LONG ZHANG[1], XINGUANG LIU[2-5], QIU-JING HE[2-5], HUILING ZHENG[2-5], SHUN XU[2-5], XING-DONG XIONG[2-5], YUAN YUAN[2-5], JIE RUAN[2,3,6], JIANG-BIN LI[2,3,6], YU XING[1], ZHONGJUN ZHOU[2,7] and SHIXIONG DENG[1]

[1]Laboratory of Forensic Medicine and Biomedical Information, College of Basic Medical Science, Chongqing Medical University, Chongqing 400016; [2]Institute of Aging Research; [3]Guangdong Provincial Key Laboratory of Medical Molecular Diagnostics, Guangdong Medical University, Dongguan, Guangdong 523808; [4]Institute of Biochemistry and Molecular Biology, Guangdong Medical University, Zhanjiang, Guangdong 524023; [5]Dongguan City Key Laboratory of Aging and Antiaging; [6]Institute of Laboratory Medicine, Guangdong Medical University, Dongguan, Guangdong 523808; [7]School of Biomedical Sciences, Li KaShing Faculty of Medicine, The University of Hong Kong, Pokfulam 999077, Hong Kong, SAR, P.R. China

Received March 16, 2017; Accepted September 27, 2017

DOI: 10.3892/mmr.2017.7731

Abstract. Cellular senescence is an irreversible growth arrest of cells that maintain their metabolic activities. Premature senescence can be induced by different stress factors and occurs in mouse embryonic fibroblasts (MEFs) derived from *Zmpste24* metalloproteinase-deficient mice, a progeria mouse model of Hutchinson-Gilford Progeria Syndrome. Previous studies have shown that miR-342-5p, an intronic microRNA (miRNA/miR) reportedly involved in ageing associated diseases, is downregulated in *Zmpste24*$^{-/-}$ MEFs. However, whether miR-342-5p is associated with the premature senescence phenotype of *Zmpste24*$^{-/-}$ MEFs remains unclear. Thus, the present study investigated the effects of miR-342-5p on cellular senescence and cell proliferation in *Zmpste24*$^{-/-}$ MEFs. The results showed that miR-342-5p overexpression ameliorated the cellular senescence phenotype to a certain extent, promoted cell proliferation and increased the G2+M cell cycle phase in *Zmpste24*$^{-/-}$ MEFs. Nonetheless, it was difficult to observe the opposite cell phenotypes in wild-type (WT) MEFs transfected with the miR-342-5p inhibitor. Growth-arrest-specific 2 (*GAS2*) was identified as a target gene of miR-342-5p in *Zmpste24*$^{-/-}$ MEFs. In addition, miR-342-5p was identified to be downregulated in WT MEFs during replicative senescence, while Gas2 was upregulated. Taken together, these findings suggest that downregulated miR-342-5p is involved in regulating cell proliferation and cell cycles in *Zmpste24*$^{-/-}$ MEFs by suppressing *GAS2 in vitro*.

Correspondence to: Professor Shixiong Deng, Laboratory of Forensic Medicine and Biomedical Information, College of Basic Medical Science, Chongqing Medical University, 1 Yixueyuan Road, Yuzhong, Chongqing 400016, P.R. China
E-mail: dengshixiong1963@163.com

Abbreviations: MEFs, mouse embryonic fibroblasts; HGPS, Hutchinson-Gilford progeria syndrome; SA-β-Gal, senescence-associated β-galactosidase; GAS2, growth-arrest-specific 2

Key words: microRNA, miR-342-5p, premature senescence, proliferation, cell cycle, *Zmpste24*, mouse embryonic fibroblasts, GAS2

Introduction

Cellular senescence is a state of stable proliferation arrest in cells and has been linked to ageing and ageing-related diseases (1). Premature senescence can be induced by many stimuli, including ionizing radiation, telomere dysfunction and reactive oxygen species (ROS) (2). Evidence indicates that premature senescence occurs in mouse embryonic fibroblasts (MEFs) derived from Zmpste24 metalloproteinase-deficient mice, a progeria mouse model of Hutchinson-Gilford Progeria Syndrome (HGPS), which is mainly caused by the accumulation of abnormal prelamin A (also known as progerin) (3-5). There are similar defects in the cellular phenotypes between progeroid cells and physiological ageing cells, such as decreased cell proliferation, increased cell senescence, altered DNA damage responses, increased genome instability, and dysregulated gene expression (6,7). It is interesting that progerin is also expressed at low levels in physiological ageing cells and is induced by telomere damage during replicative senescence in normal human fibroblasts (8-10), which implies a common mechanism between premature ageing and physiological ageing. However, the link between prelamin A accumulation and the premature senescence phenotype in *Zmpste24*$^{-/-}$ MEFs is still poorly understood.

MicroRNAs (miRNAs/miRs) are small non-coding RNAs of approximately 18~25 nucleotides that function as a negative regulator of gene expression post-transcriptionally. Recently, miRNA expression profiles and functional analyses

have revealed that miRNAs impact the premature senescence phenotype of progeroid cells (11). For instance, brain-specific miR-9 negatively controls lamin A and progerin expression in neural cells and plays a neuroprotective role in the brain (12,13). In the *Zmpste24*$^{-/-}$ progeria mouse model, the miR-29 family is involved in the DNA damage response in a p53-dependent manner (14). Our previous studies revealed that miR-365 and miR-342-5p are downregulated in *Zmpste24*$^{-/-}$ mouse embryonic fibroblasts (MEFs), in which miR-365 serves as a negative regulator of cell proliferation (15). Nevertheless, the specific roles of miRNAs in the premature senescence phenotype of progeroid cells are still largely unknown and remain to be further studied.

miR-342-5p is an intronic miRNA hosted in the Ena/Vasodilator-Stimulated Phosphoprotein-Like (Ena/VASP-like, *EVL*) gene, which belongs to the Ena/VASP family, is involved in actin cytoskeleton remodelling and reportedly potentiates ERK-sustained cell proliferation (16,17). miR-342-5p is involved in ageing-associated diseases, including Alzheimer's disease (AD) and atherosclerosis mouse models. In AD mouse models, miR-342-5p is upregulated and contributes to AD axonopathy by downregulating AnkG (18). In an *Apoe*$^{-/-}$ atherosclerosis mouse model, macrophage-derived miR-342-5p is upregulated and promotes atherosclerosis by suppressing the Akt1-mediated inhibition of miR-155 expression (19). As a downstream effector of Notch signalling, miR-342-5p regulates neural stem cell proliferation and differentiation in mice (20). These findings suggest that miR-342-5p plays different roles in different cell types. However, the role of miR-342-5p in the premature senescence phenotype of *Zmpste24*$^{-/-}$ MEFs is unclear. Here, we further investigated the function of miR-342-5p and demonstrated that miR-342-5p modulates cell proliferation and cell cycle by suppressing growth-arrest-specific 2 (*GAS2*) in *Zmpste24*$^{-/-}$ MEFs *in vitro*.

Materials and methods

Cell culture. Primary MEFs were prepared from embryonic day (E) 13.5 embryos of *Zmpste24*$^{-/-}$ and wild-type (WT) mice. All animal experiments were approved by the Committee on the Use of Live Animals in Teaching and Research (CULATR) at the University of Hong Kong and performed according to the regulation of the CULATR at the University of Hong Kong. MEFs and the mouse myoblast cell line C2C12 (obtained from Li KaShing Faculty of Medicine of the University of Hong Kong) were grown in Dulbecco's modified Eagle's medium (DMEM) (Gibco; Thermo Fisher Scientific, Inc., Waltham, MA, USA) supplemented with 10% foetal bovine serum (FBS) (Gibco; Thermo Fisher Scientific, Inc.). The cells were passaged as they reached approximately 80~90% confluency. For the replicative senescence analysis, early-passage WT MEFs (p2~p4) underwent serial passages until they reached late passage (p7~p8).

miRNA transfection. *Zmpste24*$^{-/-}$ and WT MEFs were plated in cell culture plates at a density of approximately 60~70% confluency and were incubated at 37˚C. After a 24 h incubation, the *Zmpste24*$^{-/-}$ MEFs were transiently transfected with mmu-miR-342-5p Mimics (342M) or Mimics Negative Control (NC) (50 nmol/l final), while WT MEFs were transiently transfected with 342M, NC, mmu-miR-342-5p Inhibitor (342I) or Inhibitor Negative Control (INC) (100 nmol/l final). The Mimics, NC, Inhibitor and INC were obtained from Ribobio Co., Ltd. (Guangzhou, China). Transfection was performed using the Lipofectamine® RNAiMAX Transfection Reagent (Invitrogen; Thermo Fisher Scientific, Inc.) according to the manufacturer's protocol.

Senescence-associated β-galactosidase (SA-β-Gal) staining. *Zmpste24*$^{-/-}$ and WT MEFs (p4~p5) were plated in 6-well culture plates at a density of $1.4x10^5$ cells per well and were transfected with 342M or 342I. Serial passaging was performed until the cells reached replicative senescence (p7~p8), and the transfection was reinforced at every passage. SA-β-Gal activity was detected according to the manufacturer's protocol (Beyotime Institute of Biotechnology, Shanghai, China).

MTT assay for monitoring cell growth. *Zmpste24*$^{-/-}$ and WT MEFs (p2~p4) were plated in 48-well culture plates at a density of $9x10^4$ cells per well and were transfected with 342M or 342I, and the second round of transfection was reinforced on day 3 after the first. The cells were incubated with 20 µl of MTT (5 mg/ml) (Beyotime Institute of Biotechnology) for 4 h at 37˚C on days 1, 2, 4 and 6 after the first round of transfection. The formazan crystals in the cells were solubilized with Dimethyl Sulphoxide (200 µl/well). The absorbance was measured at 490 nm using a Synergy 2 microplate reader (BioTek; Winooski, VT, USA).

EdU incorporation assay. *Zmpste24*$^{-/-}$ and WT MEFs (p2~p4) were cultured in 24-well plates and were transfected with 342M or 342I. The cell proliferation of *Zmpste24*$^{-/-}$ and WT MEFs (p2~p4) was evaluated by EdU incorporation assay 48 h after the transfection using the Cell-Light™ EdU Apollo®567 In Vitro Imaging kit (Ribobio, Guangzhou, China) following the manufacturer's protocol. The EdU positive cells were counted from at least 3 fields in every independent experiment using ImageJ2x software.

Cell cycle analysis. *Zmpste24*$^{-/-}$ and WT MEFs (p2~p4) were plated in 6-well culture plates at a density of $1.3x10^5$ cells per well. For synchronization in the G1 stage, the cells were grown in serum-free DMEM for 24 h before transfection. The cell cycle was analysed 72 h after the transfection using a FACSCanto II flow cytometer (BD Biosciences, San Jose, CA, USA). The cell cycle condition was determined using propidium iodide staining.

Protein extraction and Western blotting. Total protein was extracted 72 h after the transfection using RIPA Lysis Buffer (Beyotime Institute of Biotechnology,). The proteins were separated by SDS-polyacrylamide gel (12%) and were transferred to polyvinylidenedifluoride membranes (0.2 µm pore size) (EMD Millipore, Bellerica, MA, USA) and were then detected with a rabbit anti-p21 polyclonal antibody (sc-471, 1:600; Santa Cruz Biotechnology, Inc., Santa Cruz, CA, USA), a rabbit anti-Cdk1 monoclonal antibody (ab32384, 1:1,000; Abcam, Cambridge, MA, USA) (used to detect dephospho-Cdk1 (Tyr15) which refers to active Cdk1 signalling pathways) (21,22), a mouse

anti-Gas2 monoclonal antibody (M01, 1:1,000; Abnova, Taipei, Taiwan) and a mouse anti-α-tubulin monoclonal antibody (T5168, 1:5,000; Sigma-Aldrich; Merck KGaA, Darmstadt, Germany). The horseradish peroxidase-conjugated secondary antibodies (goat anti-rabbit IgG or anti-mouse IgG; Beyotime Institute of Biotechnology,) were diluted 3,000-fold, and the signals were detected by an enhanced chemiluminescence reagent (Pierce; Thermo Fisher Scientific, Inc.).

Construction of the luciferase reporter vector. The WT 3'-Untranslated Regions (3'-UTR) fragments (at least 500 bp) of mouse *ABCC1*, *FBXW11*, *GAS2* and *NNT*, containing the putative miR-342-5p binding sites, were amplified by polymerase chain reaction (PCR) and were cloned into the pGL3m vector, which was kindly gifted from Prof. Shi-mei Zhuang (23). The miR-342-5p predicted binding seed regions in the WT 3'-UTR of *FBXW11* and GAS2 were mutated (GCACCCCA→GC*TTT*CCA for *FBXW11*, GCACCCCA→GCA*TTT*CA for *GAS2*) by PCR and termed as mutant 3'-UTR. All the constructs were confirmed by DNA sequencing.

Dual luciferase assay. C2C12 cells were cotransfected with 40 ng of luciferase reporter vector, 20 ng of *Renilla* luciferase pRL-TK vector (Promega Corporation, Madison, WI, USA), and 342M or NC (20 nmol/l final) using Lipofectamine® 2000 (Invitrogen; Thermo Fisher Scientific, Inc.). The *Firefly* and *Renilla* luciferase activities were measured 48 h after the transfection with the Dual-Luciferase Reporter Assay System (Promega) using an FB12 Luminometer (Titertek-Berthold, Pforzheim, Germany). The *Firefly* luciferase activity was normalised to the *Renilla* luciferase activity.

RNA extraction and quantitative PCR (qPCR). Total RNA from p3 and p7 WT MEFs or the tissues from 2-month-old and 20-month-old mice or from *Zmpste24*$^{-/-}$ and WT mice was extracted using the Trizol Reagent (Invitrogen; Thermo Fisher Scientific, Inc.) according to the manufacturer's protocol. The RNA quality was assessed on an agarose gel (1%), and the RNA concentration was measured by a NanoDrop1000 spectrophotometer (NanoDrop Technologies; Thermo Fisher Scientific, Inc., Wilmington, DE, USA). For miRNA detection, the total RNA was reverse-transcribed using the All-in-One™ miRNA First-Strand cDNA Synthesis kit (GeneCopoeia, Inc., Rockville, MD, USA). qPCR was performed with All-in-One™ miRNA qPCR kit (GeneCopoeia) using a LightCycler® 96 System (Roche, Mannheim, Germany). U6 RNA was used as the internal control. For mRNA detection, total RNA was reverse-transcribed using the PrimeScript II 1st Strand cDNA Synthesis kit (Takara Bio, Inc., Otsu, Japan). qPCR was performed using the SYBR-Green Master Mix (Takara Bio, Inc.) and the following gene-specific primers: mGAS2-PF 5'-GCCTGCCAAGACCCTACCAC-3', mGAS2-PR 5'-GCAGAACCAGGCCTTCAGAT-3'; mEVL-PF 5'-AGCCACGATGAGTGAACAGAG-3', mEVL-PR 5'-TGGCAGTGTTGTGGTAGATG-3'; and mHPRT-PF 5'-AGGGATTTGAATCACGTTTG-3', mHPRT-PR 5'-TTACTGGCAACATCAACAGG-3'. *HPRT* was used as a housekeeping gene for normalization. Relative expression levels were analysed using the $2^{-\Delta\Delta Cq}$ method as described (24).

Statistical analysis. All the values were shown as the mean ± standard deviation from at least three independent experiments unless otherwise indicated. The non-parametric Mann-Whitney test was used to compare the percentage of SA-β-Gal positive cells between two groups. In other cases, statistical significance was determined using a two-tailed Student's t-test (α=0.05).

Results

miR-342-5p overexpression ameliorated the cellular senescence phenotype to some extent in Zmpste24$^{-/-}$ *MEFs*. Since miR-342-5p was significantly downregulated in premature senescent *Zmpste24*$^{-/-}$ MEFs (15), we further investigated the expression of miR-342-5p in WT MEFs during replicative senescence and in tissues from physiological ageing mice and *Zmpste24*$^{-/-}$ progeroid mice. Our data showed that miR-342-5p was downregulated in MEFs during replicative senescence as well (at least 5-folds, P<0.01) (Fig. 1A). However, no significant differences were observed in the expression of miR-342-5p in several tissues from physiological ageing mice (Fig. 1B) or from *Zmpste24*$^{-/-}$ progeroid mice (Fig. 1C). The mRNA expression of the *EVL* host gene was also not consistent with the expression of miR-342-5p in several tissues from *Zmpste24*$^{-/-}$ mice compared with WT mice (Fig. 1D). Next, we further sought to explore whether miR-342-5p overexpression rescued the cellular senescence phenotype in *Zmpste24*$^{-/-}$ MEFs. As shown in Fig. 1E and F, miR-342-5p overexpression decreased the percentage of SA-β-Gal staining positive cells (one characteristic of cellular senescence) in *Zmpste24*$^{-/-}$ MEFs. Moreover, the large flattened cell morphology, another characteristic of cellular senescence, was also improved to some degree in *Zmpste24*$^{-/-}$ MEFs transfected with 342M (Fig. 1E). In addition, we performed parallel experiments in WT MEFs transfected with 342I (single-stranded antisense RNA). Nonetheless, the cellular senescence phenotype was hardly affected in WT MEFs when miR-342-5p was suppressed (data not shown). Meanwhile, we detected the expression level of miR-342-5p and found that the miR-342-5p expression level in 342M transfected group was at least $1x10^4$-fold higher than that in NC transfected group, while the miR-342-5p expression level in 342I transfected group was hardly affected compared with that in INC transfected group (data not shown). Here, the 342I could inhibit miR-342-5p without inducing the degradation of miR-342-5p. Therefore, these results were in line with expectations and conformed that the transfection of 342I or 342M worked fine.

miR-342-5p overexpression promoted cell proliferation in Zmpste24$^{-/-}$ *and WT MEFs*. To investigate the effect of miR-342-5p on cell proliferation in *Zmpste24*$^{-/-}$ MEFs, we first evaluated cell viability by an MTT Assay. As shown in Fig. 2A, the overexpression of miR-342-5p increased cell viability in *Zmpste24*$^{-/-}$ MEFs. However, cell viability was not affected in WT MEFs transfected with 342I (Fig. 2B). Next, we evaluated cell proliferation in *Zmpste24*$^{-/-}$ and WT MEFs by the EdU incorporation assay. Consistent with the results of the MTT Assay, the overexpression of miR-342-5p increased the EdU positive cells in *Zmpste24*$^{-/-}$ and WT MEFs (increased by ~50%, P<0.05), while the suppression of miR-342-5p minimally affected cell proliferation in WT MEFs (Fig. 2C-F). Collectively,

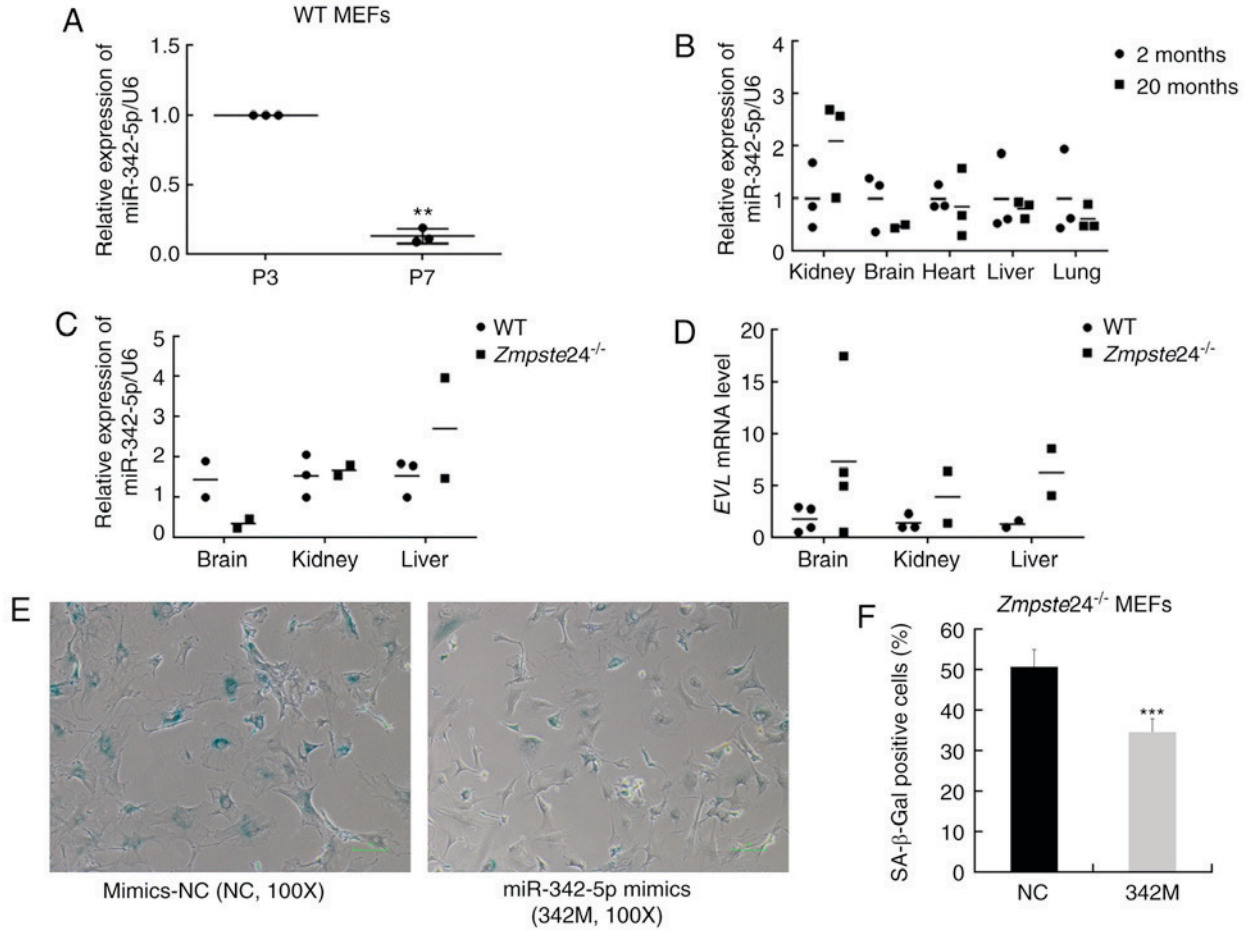

Figure 1. Overexpression of miR-342-5p decreased SA-β-Gal staining in *Zmpste24*$^{-/-}$ mouse embryonic fibroblasts (MEFs). (A) qPCR was used to detect the expression of mmu-miR-342-5p in WT MEFs during replicative senescence. n=3 independent experiments, **P<0.01 (paired Student's t-test). (B) The relative expression of mmu-miR-342-5p in the kidney, brain, heart, liver and lung from 2-month-old mice (n=3) and 20-month-old mice (n=3). (C) The relative expression of mmu-miR-342-5p in the brain, kidney and liver from WT mice (n=3) and *Zmpste24*$^{-/-}$ mice (n=3) (extreme outliers were eliminated for high $C_{quantification}$ cycle (Cq) values in the qPCR). (D) *EVL* mRNA level in the brain, kidney and liver from WT mice (n=4) and *Zmpste24*$^{-/-}$ mice (n=4) (extreme outliers were eliminated for high Cq values in the qPCR). (E) Representative images of the SA-β-Gal staining in *Zmpste24*$^{-/-}$ MEFs. Original magnification, x100. (F) The percentage of SA-β-Gal positive cells is shown in the histogram, which corresponds to the means ± standard error of the mean (SEM) (bars) of at least 1,800 cells or 33 random fields pooled from independent experiments, ***P<0.001 (Mann-Whitney tests).

these results suggest that miR-342-5p overexpression promotes *Zmpste24*$^{-/-}$ and WT MEFs proliferation.

miR-342-5p overexpression increased the G2+M cell cycle phase in Zmpste24$^{-/-}$ *and WT MEFs*. Since miR-342-5p overexpression promotes cell proliferation in *Zmpste24*$^{-/-}$ and WT MEFs, we further investigated the effects of miR-342-5p on cell cycle in *Zmpste24*$^{-/-}$ and WT MEFs. Our data showed that the overexpression of miR-342-5p increased the G2+M cell cycle phase and decreased the S phase in *Zmpste24*$^{-/-}$ and WT MEFs (Fig. 3A-D). However, the cell cycle was not affected in WT MEFs transfected with 342I compared with INC (Fig. 3C-D). Since $p21^{CIP1/WAF1}$ and Cdk1 (cdc2) are key regulators in the progression of the G2/M phase (22,25,26), we further investigated the protein levels of $p21^{CIP1/WAF1}$ and Cdk1 in *Zmpste24*$^{-/-}$ and WT MEFs. The Western blot results indicated that the overexpression of miR-342-5p increased the protein level of Cdk1 in *Zmpste24*$^{-/-}$ MEFs (Fig. 3E). Collectively, these results suggested that miR-342-5p overexpression increased the G2/M phase, likely via upregulating Cdk1 in *Zmpste24*$^{-/-}$ MEFs.

GAS2 is a target gene of miR-342-5p. To identify the direct target genes of miR-342-5p in *Zmpste24*$^{-/-}$ MEFs, we selected several potential target genes via 4 target prediction algorithms *in silico* (Table I). Then, we carried out the Dual luciferase assay to assess whether miR-342-5p binds to the 3'UTR of these potential target genes *in vitro*. Since it was difficult to perform the transfection with the luciferase vectors due to the low transfection efficiency in the MEFs, we performed the Dual luciferase assay in C2C12 cells, which is a mouse myoblast cell line with high efficiency for gene transfection. As shown in Fig. 4A, miR-342-5p significantly inhibited the firefly luciferase activity of the WT 3'UTR of *FBXW11* and *GAS2*. Next, we mutated the seed binding site in the WT 3'UTR of *FBXW11* (GC<u>ACC</u>CCA→GC<u>*TTT*</u>CCA) and *GAS2* (GCA<u>CCC</u>CA→GCA<u>*TTT*</u>CA) (Fig. 4B). Our data showed that the *GAS2* mutant 3'UTR restored the luciferase activity (Fig. 4C). We further checked the Gas2 protein level in WT and *Zmpste24*$^{-/-}$ MEFs (p2~p4) transfected with 342I or 342M. As shown in Fig. 4D, the overexpression of miR-342-5p downregulated Gas2 in *Zmpste24*$^{-/-}$ MEFs, while the inhibition of miR-342-5p upregulated Gas2 in WT MEFs. Taken together,

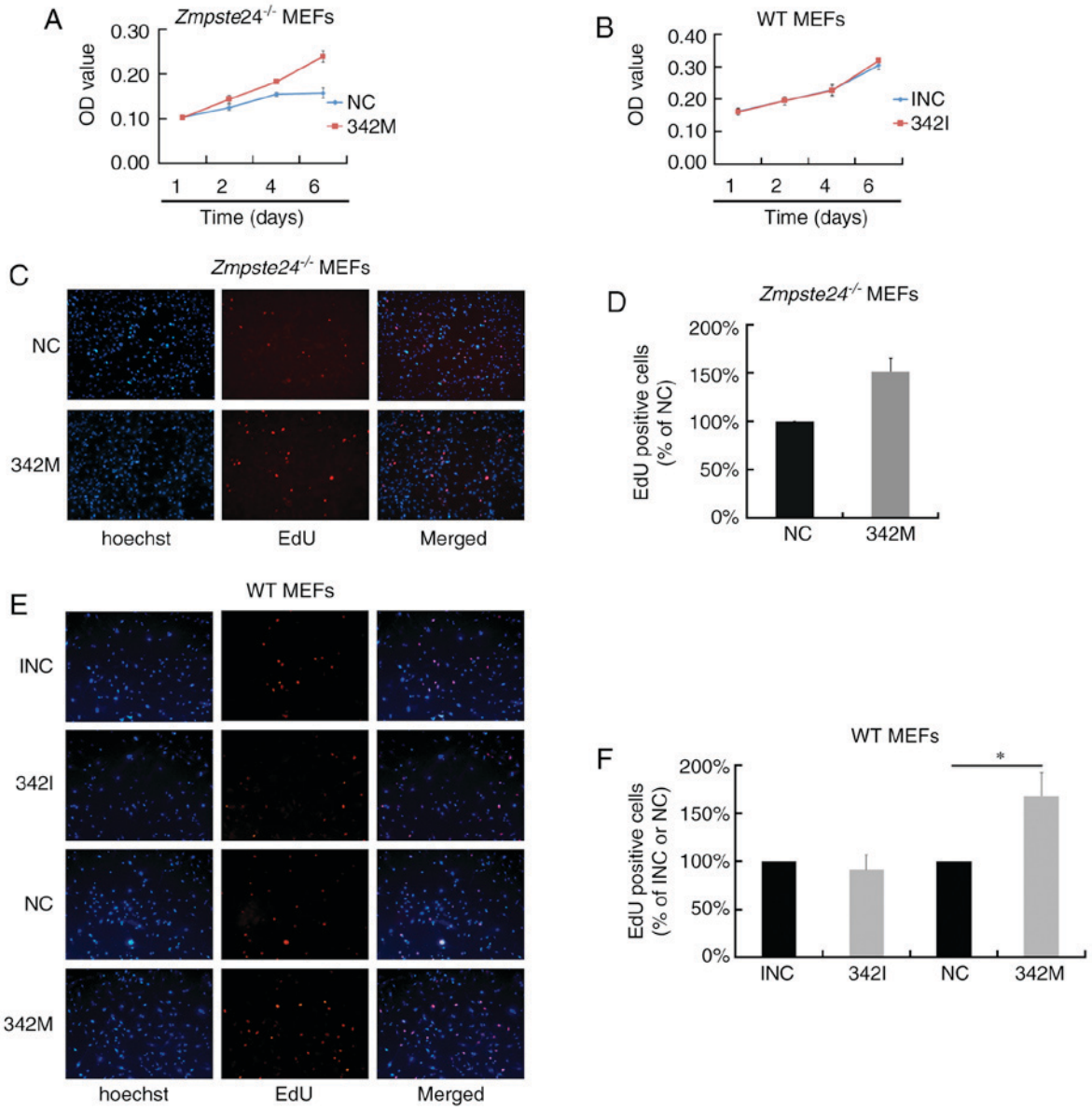

Figure 2. Overexpression of miR-342-5p promoted *Zmpste24*$^{-/-}$ and wild-type (WT) mouse embryonic fibroblasts (MEFs) proliferation. (A and B) Cell viability in *Zmpste24*$^{-/-}$ and WT MEFs. Representative results of one independent experiment are presented. The values are shown as the means ± SD (bars) (n=4 biological replicates from separate wells), and at least three independent experiments were performed. (C) Representative images of the EdU positive cells in *Zmpste24*$^{-/-}$ MEFs. Original magnification, x100. (D) The results of the EdU positive cells in *Zmpste24*$^{-/-}$ MEFs are presented as a histogram. The values are shown as the means ± SD (bars) (n=3 independent experiments), *P<0.05 (paired Student's t-test). (E) Representative images of the EdU positive cells in WT MEFs. Original magnification, x100. (F) The results of the EdU positive cells in WT MEFs are presented as a histogram. The values are shown as the means ± SD (bars) (n=3 independent experiments), *P<0.05 (paired Student's t-test).

these results demonstrated that miR-342-5p downregulated *GAS2* by directly binding to the 3'UTR of *GAS2* mRNA in *Zmpste24*$^{-/-}$ MEFs. We further investigated whether *GAS2* is dysregulated in WT MEFs during replicative senescence or in tissues from physiological ageing mice or from *Zmpste24*$^{-/-}$ progeroid mice. As shown in Fig. 4E, the Gas2 protein level was upregulated in WT MEFs during replicative senescence. Moreover, the *GAS2* mRNA level was upregulated in the kidney of ageing mice as well (Fig. 4F).

Discussion

Increasing evidence shows that miRNAs play important roles in the premature cell senescence phenotypes of progeroid cells; however, the functions of most miRNAs are still unclear. Previous studies show that miR-342-5p is downregulated in *Zmpste24*$^{-/-}$ progeroid MEFs (15). We herein revealed that miR-342-5p overexpression was sufficient to promote *Zmpste24*$^{-/-}$ MEFs proliferation and ameliorated the senescence phenotype to some extent, which provides novel insights into the role of miR-342-5p in the premature senescence phenotypes of *Zmpste24*$^{-/-}$ MEFs.

miR-342-5p, an intronic miRNA hosted in the *EVL* gene, is reportedly dysregulated in ageing-associated diseases, such as Alzheimer's disease and atherosclerosis mouse models (18,19). In this research, we found that miR-342-5p was downregulated in WT MEFs during replicative senescence (Fig. 1A), which is consistent with the downregulation in premature senescence

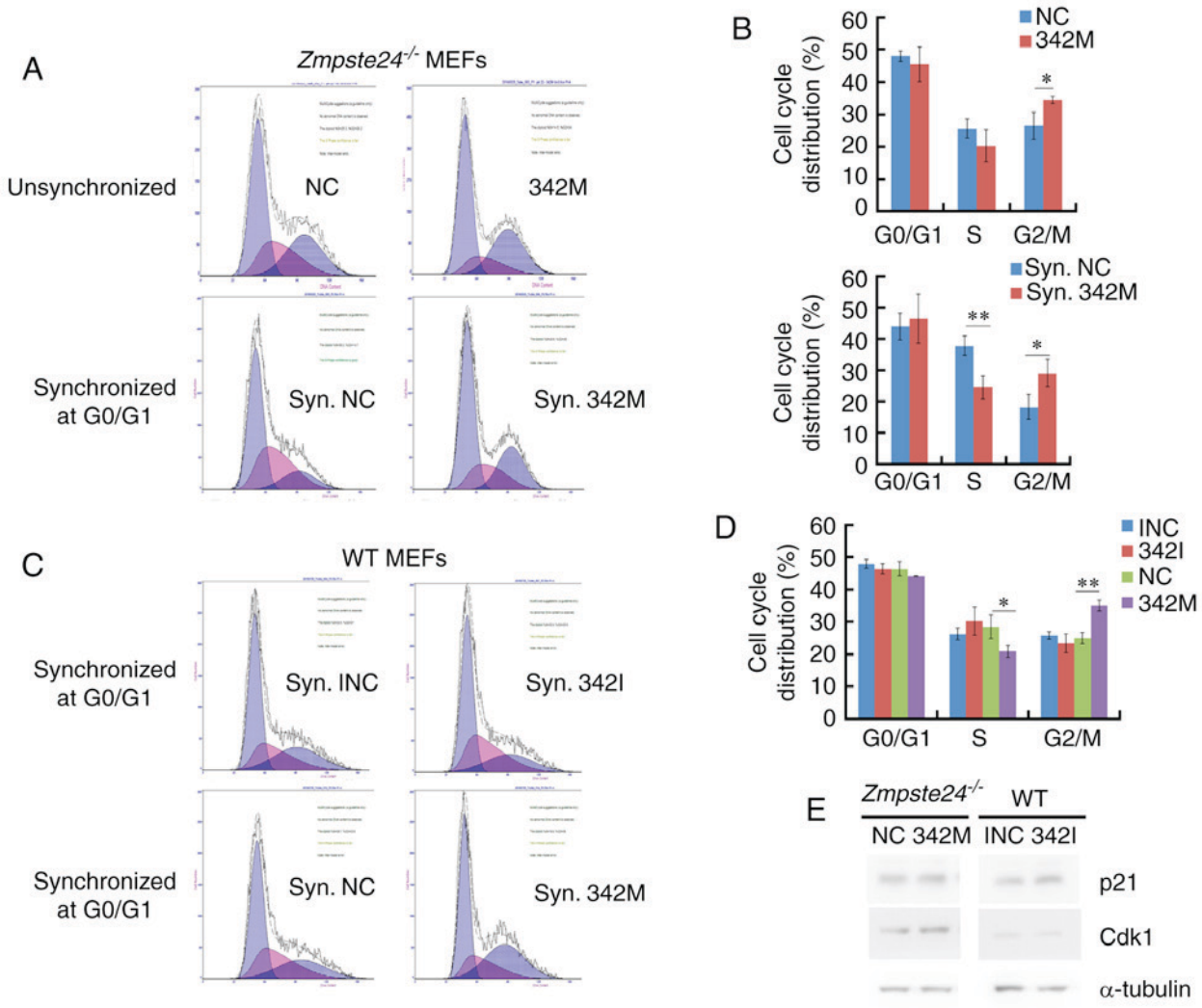

Figure 3. Overexpression of miR-342-5p increased the G2+M cell cycle phase in *Zmpste24*$^{-/-}$ and wild-type (WT) mouse embryonic fibroblasts (MEFs). (A and B) Cell cycle analysis of *Zmpste24*$^{-/-}$ MEFs. Top panel: unsynchronized *Zmpste24*$^{-/-}$ MEFs; bottom panel: synchronized *Zmpste24*$^{-/-}$ MEFs. The histogram shows the percentage of cell cycle distribution. The values are shown as the means ± SD (bars) (n=3 independent experiments), *P<0.05, **P<0.01 (unpaired Student's t-test). (C and D) Cell cycle analysis of WT MEFs (synchronized). Representative results of one independent experiment are presented. The values are shown as the means ± SD (bars) (n=3 biological replicates from separate wells), and at least three independent experiments were performed. (E) Western blotting was used to detect the expression of p21 and Cdk1 in *Zmpste24*$^{-/-}$ and WT MEFs.

of *Zmpste24*$^{-/-}$ MEFs (15). However, we did not observe a significant dysregulation of miR-342-5p in several tissues from physiological ageing mice or from *Zmpste24*$^{-/-}$ progeroid mice (Fig. 1B-C), which may be due to the small number of investigated specimens or due to different cell backgrounds: the tissue cells are terminally differentiated cells which is different from the MEFs, thus the gene expression pattern of senescent MEFs (replicative senescence) is not always consistent with that of (premature) ageing tissues. In human colorectal cancer and inflammatory breast cancer, a downregulation of miR-342-5p is an epigenetic silencing mechanism due to the CpG island methylation upstream of *EVL* (27,28). However, the expression of miR-342-5p was not consistent with that of *EVL* mRNA in several tissues from *Zmpste24*$^{-/-}$ mice (Fig. 1C-D). Indeed, the small sample number is a limitation of the present study, and it is necessary to repeat these tests with more samples in future studies.

For the cell phenotype analyses, we first tested the effects of miR-342-5p on cellular senescence and found that miR-342-5p overexpression ameliorated the senescence phenotype in *Zmpste24*$^{-/-}$ MEFs to some extent (Fig. 1E-F). Hence, we speculated that miR-342-5p might be involved in regulating cell proliferation or cell cycle in *Zmpste24*$^{-/-}$ MEFs. Indeed, miR-342-5p overexpression was sufficient to promoted cell proliferation in *Zmpste24*$^{-/-}$ and WT MEFs (Fig. 2). However, our results are not in agreement with a recent report that miR-342-5p overexpression inhibits endothelial cell proliferation (29). At first glance, such results may seem contradictory, but it is worth noting that miRNAs can have different effects in different cell types (30,31).

Next, we investigated the effects of miR-342-5p on the cell cycle and found that miR-342-5p overexpression increased the G2+M cell cycle phase in both *Zmpste24*$^{-/-}$ and WT MEFs. In addition, miR-342-5p overexpression upregulated Cdk1 in *Zmpste24*$^{-/-}$ MEFs (Fig. 3). In the cell cycle, Cdk1 is required for the entry of all eukaryotic cells into mitosis (22,32) and is sufficient to drive the mammalian cell cycle (33). Hence, miR-342-5p overexpression promotes cell proliferation

Table I. Potential target genes of mmu-miR-342-5p predicted by target prediction algorithms.

	TargetScan	miRanda	MicroCosm	miRDB
ABCC1	√	√	√	√
FBXW11	√	√	√	
GAS2	√	√		√
NNT	√	√		√

TargetScan (http://www.targetscan.org/); miRanda (http://www.microrna.org/); MicroCosm (http://www.ebi.ac.uk/enright-srv/microcosm/htdocs/targets/v5/); miRDB (http://www.mirdb.org/).

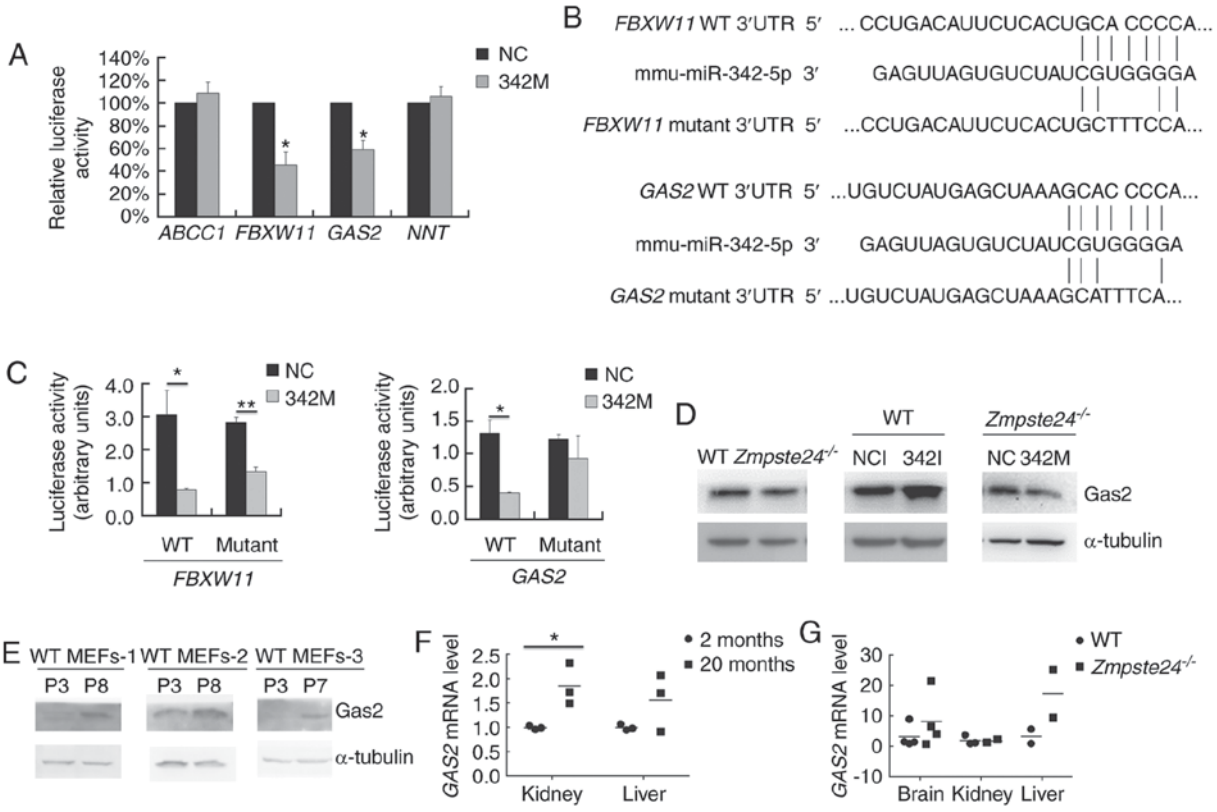

Figure 4. *GAS2* was a target of miR-342-5p. (A) The results of the Dual luciferase assay of the wild-type (WT) 3'UTR of the potential target genes. The values are shown as the means ± SD (bars) (n=3 independent experiments), *P<0.05 (paired Student's t-test). (B) *FBXW11*/*GAS2* WT and mutant 3'UTR seed binding site of mmu-miR-342-5p. (C) The results of the Dual luciferase assay of the *FBXW11*/*GAS2* WT and mutant 3'UTR. The values are shown as the means ± SD (bars) (n=3 independent experiments), *P<0.05, **P<0.01 (unpaired Student's t-test). (D) Western blotting was used to detect Gas2 expression in *Zmpste24*$^{-/-}$ and WT mouse embryonic fibroblasts (MEFs). (E) Western blotting was used to detect Gas2 expression in WT MEFs during replicative senescence. (F) qPCR was used to quantify the *GAS2* mRNA level in the kidney and liver from 2-month-old mice (n=3) and 20-month-old mice (n=3). The values are shown as the means ± SD (bars), *P<0.05 (unpaired Student's t-test). (G) The *GAS2* mRNA level in the brain, kidney and liver from WT mice (n=4) and *Zmpste24*$^{-/-}$ mice (n=4) (extreme outliers were eliminated for high Cq values in the qPCR).

probably by upregulating Cdk1 in *Zmpste24*$^{-/-}$ MEFs. Since p21$^{CIP1/WAF1}$ serves as a negative regulator in the G2/M transition (25,26) and plays a critical role in cellular senescence, we speculated that miR-342-5p might upregulate Cdk1 through the inhibition of p21$^{CIP1/WAF1}$. However, it was difficult to observe a consistent suppression of p21$^{CIP1/WAF1}$ when overexpressing miR-342-5p in *Zmpste24*$^{-/-}$ MEFs.

Of note, as we carried out a loss-of-function analysis by transfection with the miR-342-5p Inhibitor (single-stranded antisense siRNA) in WT MEFs, and it was difficult to observe the opposite cell phenotypes, such as cellular senescence, cell proliferation, and cell cycle when compared with miR-342-5p overexpression. One possible reason may be due to the extremely low basal expression of miR-342-5p in WT MEFs. Another possible reason may be that there is not only one miRNA that regulates cell phenotypes, and thus, if we suppressed all the related miRNAs at the same time, it is possible that the significant phenotypes of the loss-of-function could be easily observed.

Additionally, we further identified *GAS2* as a target gene of miR-342-5p in *Zmpste24*$^{-/-}$ MEFs (Fig. 4A-D). Gas2 was originally identified in growth arrested mouse fibroblasts (34)

and inhibits cell division in *Xenopus* embryos (35). As a p53-stabilizing protein, Gas2 is implicated in p53-induced growth inhibition (36). In *4E-BP1*$^{-/-}$*4E-BP2*$^{-/-}$ double knockout MEFs, the suppression of Gas2 by shRNA reduces the SA-β-Gal activity and increases proliferation, demonstrating that Gas2 expression is a prerequisite for cellular senescence (37). In this research, we found that Gas2 was upregulated in WT MEFs during replicative senescence (Fig. 4E), and *GAS2* mRNA was upregulated in kidney of ageing mice (Fig. 4F). Taken together, these results indicate that miR-342-5p promotes *Zmpste24*$^{-/-}$ MEFs proliferation by suppressing *GAS2*.

Generally, the present study mainly focused at the cell level, thus it can not confirm that the miR-342-5p has an effect on the cellular senescence in *Zmpste24*$^{-/-}$ MEFs *in vivo*. The validation test *in vivo* from animals remains to be further investigated. In conclusion, our data suggest that downregulated miR-342-5p is involved in regulating cell proliferation and the cell cycle via suppressing *GAS2* in *Zmpste24*$^{-/-}$ MEFs *in vitro*, which may have implications for the underlying mechanisms of premature senescence in progeroid cells.

Acknowledgements

We are grateful to Professor Yousin Suh (Albert Einstein College of Medicine, Bronx, NY, USA), Professor Brian K. Kennedy (Buck Institute for Research on Aging, Novato, CA, USA) and Professor Matt Kaeberlein (University of Washington, Seattle, WA, USA) for their technical assistance and discussion. We would also like to thank American Journal Experts for English language editing. This study was supported by the National Natural Science Foundation of China (nos. 81170327, 81671399, 31600976 and 81202385), the Ordinary University Innovation Team Construction Project of Guangdong Province (no. 2015KCXTD022), and the Dongguan International Science and Technology Cooperation (including Hong Kong, Macao and Taiwan) Project (no. 201650812001).

References

1. McCulloch K, Litherland GJ and Rai TS: Cellular senescence in osteoarthritis pathology. Aging Cell 16: 210-218, 2017.
2. Khan SY, Awad EM, Oszwald A, Mayr M, Yin X, Waltenberger B, Stuppner H, Lipovac M, Uhrin P and Breuss JM: Premature senescence of endothelial cells upon chronic exposure to TNFα can be prevented by N-acetyl cysteine and plumericin. Sci Rep 7: 39501, 2017.
3. Liu B, Wang J, Chan KM, Tjia WM, Deng W, Guan X, Huang JD, Li KM, Chau PY, Chen DJ, *et al*: Genomic instability in laminopathy-based premature aging. Nat Med 11: 780-785, 2005.
4. Eriksson M, Brown WT, Gordon LB, Glynn MW, Singer J, Scott L, Erdos MR, Robbins CM, Moses TY, Berglund P, *et al*: Recurrent de novo point mutations in laminA cause Hutchinson-Gilford progeria syndrome. Nature 423: 293-298, 2003.
5. Pendás AM, Zhou Z, Cadiñanos J, Freije JM, Wang J, Hultenby K, Astudillo A, Wernerson A, Rodríguez F, Tryggvason K and López-Otín C: Defective prelamin A processing and muscular and adipocyte alterations in Zmpste24 metalloproteinase-deficient mice. Nat Genet 31: 94-99, 2002.
6. Goldman RD, Shumaker DK, Erdos MR, Eriksson M, Goldman AE, Gordon LB, Gruenbaum Y, Khuon S, Mendez M, Varga R and Collins FS: Accumulation of mutant lamin A causes progressive changes in nuclear architecture in Hutchinson-Gilford progeria syndrome. Proc Natl Acad Sci USA 101: 8963-8968, 2004.
7. Barthélémy F, Navarro C, Fayek R, Da Silva N, Roll P, Sigaudy S, Oshima J, Bonne G, Papadopoulou-Legbelou K, Evangeliou AE, *et al*: Truncated prelaminA expression in HGPS-like patients: A transcriptional study. Eur J Hum Genet 23: 1051-1061, 2015.
8. Olive M, Harten I, Mitchell R, Beers JK, Djabali K, Cao K, Erdos MR, Blair C, Funke B, Smoot L, *et al*: Cardiovascular pathology in Hutchinson-Gilford progeria: Correlation with the vascular pathology of aging. Arterioscler Thromb Vascr Biol 30: 2301-2309, 2010.
9. Scaffidi P and Misteli T: Lamin A-dependent nuclear defects in human aging. Science 312: 1059-1063, 2006.
10. Cao K, Blair CD, Faddah DA, Kieckhaefer JE, Olive M, Erdos MR, Nabel EG and Collins FS: Progerin and telomere dysfunction collaborate to trigger cellular senescence in normal human fibroblasts. J Clin Invest 121: 2833-2844, 2011.
11. Arancio W, Pizzolanti G, Genovese SI, Pitrone M and Giordano C: Epigenetic involvement in Hutchinson-Gilford progeria syndrome: A mini-review. Gerontology 60: 197-203, 2014.
12. Jung HJ, Coffinier C, Choe Y, Beigneux AP, Davies BS, Yang SH, Barnes RH II, Hong J, Sun T, Pleasure SJ, *et al*: Regulation of prelamin A but not lamin C by miR-9, a brain-specific microRNA. Proc Natl Acad Sci USA 109: E423-E431, 2012.
13. Nissan X, Blondel S, Navarro C, Maury Y, Denis C, Girard M, Martinat C, De Sandre-Giovannoli A, Levy N and Peschanski M: Unique preservation of neural cells in Hutchinson-Gilford progeria syndrome is due to the expression of the neural-specific miR-9 microRNA. Cell Rep 2: 1-9, 2012.
14. Ugalde AP, Ramsay AJ, de la Rosa J, Varela I, Mariño G, Cadiñanos J, Lu J, Freije JM and López-Otín C: Aging and chronic DNA damage response activate a regulatory pathway involving miR-29 and p53. EMBO J 30: 2219-2232, 2011.
15. Xiong XD, Jung HJ, Gombar S, Park JY, Zhang CL, Zheng H, Ruan J, Li JB, Kaeberlein M, Kennedy BK, *et al*: MicroRNA transcriptome analysis identifies miR-365 as a novel negative regulator of cell proliferation in Zmpste24-deficient mouse embryonic fibroblasts. Mutat Res 777: 69-78, 2015.
16. Bear JE, Svitkina TM, Krause M, Schafer DA, Loureiro JJ, Strasser GA, Maly IV, Chaga OY, Cooper JA, Borisy GG and Gertler FB: Antagonism between Ena/VASP proteins and actin filament capping regulates fibroblast motility. Cell 109: 509-521, 2002.
17. Tavares S, Vieira AF, Taubenberger AV, Araújo M, Martins NP, Brás-Pereira C, Polónia A, Herbig M, Barreto C, Otto O, *et al*: Actin stress fiber organization promotes cell stiffening and proliferation of pre-invasive breast cancer cells. Nat Commun 8: 15237, 2017.
18. Sun X, Wu Y, Gu M and Zhang Y: miR-342-5p decreases ankyrin G levels in Alzheimer's disease transgenic mouse models. Cell Rep 6: 264-270, 2014.
19. Wei Y, Nazari-Jahantigh M, Chan L, Zhu M, Heyll K, Corbalán-Campos J, Hartmann P, Thiemann A, Weber C and Schober A: The microRNA-342-5p fosters inflammatory macrophage activation through an Akt1- and microRNA-155-dependent pathway during atherosclerosis. Circulation 127: 1609-1619, 2013.
20. Gao F, Zhang YF, Zhang ZP, Fu LA, Cao XL, Zhang YZ, Guo CJ, Yan XC, Yang QC, Hu YY, *et al*: miR-342-5p regulates neural stem cell proliferation and differentiation downstream to Notch signaling in mice. Stem Cell Reports 8: 1032-1045, 2017.
21. Wang J, Zhang Y, Xu S, Li W, Chen Z, Wang Z, Han X, Zhao Y and Li S: Prognostic significance of G2/M arrest signaling pathway proteins in advanced non-small cell lung cancer patients. Oncol Lett 9: 1266-1272, 2015.
22. Fesquet D, Labbé JC, Derancourt J, Capony JP, Galas S, Girard F, Lorca T, Shuttleworth J, Dorée M and Cavadore JC: The MO15 gene encodes the catalytic subunit of a protein kinase that activates cdc2 and other cyclin-dependent kinases (CDKs) through phosphorylation of Thr161 and its homologues. EMBO J 12: 3111-3121, 1993.
23. Su H, Yang JR, Xu T, Huang J, Xu L, Yuan Y and Zhuang SM: MicroRNA-101, down-regulated in hepatocellular carcinoma, promotes apoptosis and suppresses tumorigenicity. Cancer Res 69: 1135-1142, 2009.
24. Livak KJ and Schmittgen TD: Analysis of relative gene expression data using real-time quantitative PCR and the 2(-Delta DeltaC(T)) Method. Methods 25: 402-408, 2001.
25. Niculescu AB III, Chen X, Smeets M, Hengst L, Prives C and Reed SI: Effects of p21(Cip1/Waf1) at both the G1/S and the G2/M cell cycle transitions: pRb is a critical determinant in blocking DNA replication and in preventing endoreduplication. Mol Cell Biol 18: 629-643, 1998.

26. Barboule N, Lafon C, Chadebech P, Vidal S and Valette A: Involvement of p21 in the PKC-induced regulation of the G2/M cell cycle transition. FEBS Lett 444: 32-37, 1999.
27. Grady WM, Parkin RK, Mitchell PS, Lee JH, Kim YH, Tsuchiya KD, Washington MK, Paraskeva C, Willson JK, Kaz AM, *et al*: Epigenetic silencing of the intronic microRNA hsa-miR-342 and its host gene EVL in colorectal cancer. Oncogene 27: 3880-3888, 2008.
28. Van der Auwera I, Yu W, Suo L, Van Neste L, van Dam P, Van Marck EA, Pauwels P, Vermeulen PB, Dirix LY and Van Laere SJ: Array-based DNA methylation profiling for breast cancer subtype discrimination. PLoS One 5: e12616, 2010.
29. Yan XC, Cao J, Liang L, Wang L, Gao F, Yang ZY, Duan JL, Chang TF, Deng SM, Liu Y, *et al*: miR-342-5p is a Notch downstream molecule and regulates multiple angiogenic pathways including Notch, vascular endothelial growth factor and transforming growth factor β signaling. J Am Heart Assoc 5: e003042, 2016.
30. Calin GA and Croce CM: MicroRNA signatures in human cancers. Nat Rev Cancer 6: 857-866, 2006.
31. Esquela-Kerscher A and Slack FJ: Oncomirs - microRNAs with a role in cancer. Nat Rev Cancer 6: 259-269, 2006.
32. Peter M, Le Peuch C, Labbé JC, Meyer AN, Donoghue DJ and Doree M: Initial activation of cyclin-B1-cdc2 kinase requires phosphorylation of cyclin B1. EMBO Rep 3: 551-556, 2002.
33. Santamaría D, Barrière C, Cerqueira A, Hunt S, Tardy C, Newton K, Cáceres JF, Dubus P, Malumbres M and Barbacid M: Cdk1 is sufficient to drive the mammalian cell cycle. Nature 448: 811-815, 2007.
34. Schneider C, King RM and Philipson L: Genes specifically expressed at growth arrest of mammalian cells. Cell 54: 787-793, 1988.
35. Zhang T, Dayanandan B, Rouiller I, Lawrence EJ and Mandato CA: Growth-arrest-specific protein 2 inhibits cell division in Xenopus embryos. PLoS One 6: e24698, 2011.
36. Kondo Y, Shen L, Cheng AS, Ahmed S, Boumber Y, Charo C, Yamochi T, Urano T, Furukawa K, Kwabi-Addo B, *et al*: Gene silencing in cancer by histone H3 lysine 27 trimethylation independent of promoter DNA methylation. Nat Genet 40: 741-750, 2008.
37. Petroulakis E, Parsyan A, Dowling RJ, LeBacquer O, Martineau Y, Bidinosti M, Larsson O, Alain T, Rong L, Mamane Y, *et al*: p53-dependent translational control of senescence and transformation via 4E-BPs. Cancer Cell 16: 439-446, 2009.